

PRISM: A Unified Framework for Photorealistic Reconstruction and Intrinsic Scene Modeling

ALARA DIRIK, Imperial College London, United Kingdom
 TUANFENG WANG, Adobe Research, United Kingdom
 DUYGU CEYLAN, Adobe Research, United Kingdom
 STEFANOS ZAFEIRIOU, Imperial College London, United Kingdom
 ANNA FRÜHSTÜCK, Adobe Research, United Kingdom

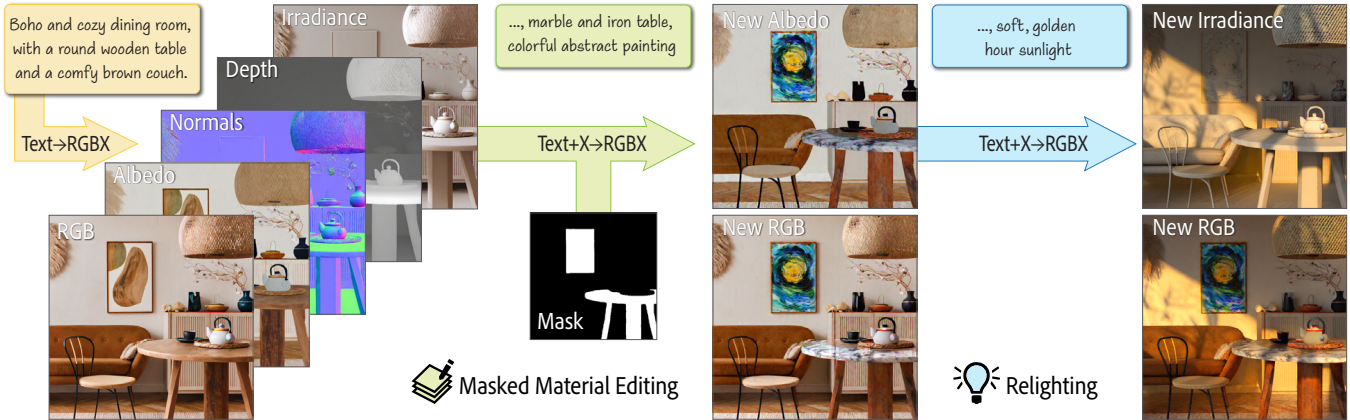


Fig. 1. We propose PRISM, a unified framework for conditional generation of RGB image and its intrinsic channels (referred to as X layers) simultaneously. It supports a variety of tasks, including text-to-RGBX generation, RGB-to-X decomposition, and X-to-RGBX conditional generation. PRISM achieves plausible results on both local material editing on masked region and global image relighting through conditioning on selected intrinsic layers and text prompts.

We present PRISM, a unified framework that enables multiple image generation and editing tasks in a single foundational model. Starting from a pre-trained text-to-image diffusion model, PRISM proposes an effective fine-tuning strategy to produce RGB images along with intrinsic maps (referred to as X layers) simultaneously. Unlike previous approaches, which infer intrinsic properties individually or require separate models for decomposition and conditional generation, PRISM maintains consistency across modalities by generating all intrinsic layers jointly. It supports diverse tasks, including text-to-RGBX generation, RGB-to-X decomposition, and X-to-RGBX conditional generation. Additionally, PRISM enables both global and local image editing through conditioning on selected intrinsic layers and text prompts. Extensive experiments demonstrate the competitive performance of PRISM both for intrinsic image decomposition and conditional image generation while preserving the base model's text-to-image generation capability.

Authors' addresses: Alara Dirik, a.dirik22@imperial.ac.uk, Imperial College London, United Kingdom; Tuanfeng Wang, yangtuan@adobe.com, Adobe Research, United Kingdom; Duygu Ceylan, ceylan@adobe.com, Adobe Research, United Kingdom; Stefanos Zafeiriou, s.zafeiriou@imperial.ac.uk, Imperial College London, United Kingdom; Anna Frühstück, fruehstu@adobe.com, Adobe Research, United Kingdom.

Permission to make digital or hard copies of all or part of this work for personal or classroom use is granted without fee provided that copies are not made or distributed for profit or commercial advantage and that copies bear this notice and the full citation on the first page. Copyrights for components of this work owned by others than ACM must be honored. Abstracting with credit is permitted. To copy otherwise, or republish, to post on servers or to redistribute to lists, requires prior specific permission and/or a fee. Request permissions from permissions@acm.org.

© 2025 Association for Computing Machinery.

0730-0301/2025/5-ART \$15.00

<https://doi.org/10.1145/nnnnnnn.nnnnnnn>

CCS Concepts: • Computing methodologies → Rendering; Image processing.

Additional Key Words and Phrases: Diffusion models, intrinsic decomposition, realistic rendering

ACM Reference Format:

Alara Dirik, Tuanfeng Wang, Duygu Ceylan, Stefanos Zafeiriou, and Anna Frühstück. 2025. PRISM: A Unified Framework for Photorealistic Reconstruction and Intrinsic Scene Modeling. *ACM Trans. Graph.* 1, 1 (May 2025), 14 pages. <https://doi.org/10.1145/nnnnnnn.nnnnnnn>

1 INTRODUCTION

Foundational image generation models have seen significant advances recently enabling high quality image generation from text descriptions [Chen et al. 2023; Ramesh et al. 2022]. Such models have also been extended for various image editing as well as more explicit conditional generation workflows. Motivated by such rapid success, recent work have proposed to benefit from the generative prior of such models for various perception tasks including depth [Ke et al. 2024] and normal [Ye et al. 2024] estimation as well as intrinsic image decomposition [Kocsis et al. 2024; Luo et al. 2024a; Zeng et al. 2024]. Such methods often finetune a pre-trained image generation model, effectively replacing the image generation capability with the ability to predict a certain spatial map from a given input image.

We argue that perceiving an image as a composition of its intrinsic components (albedo, shading, and geometric properties) is a

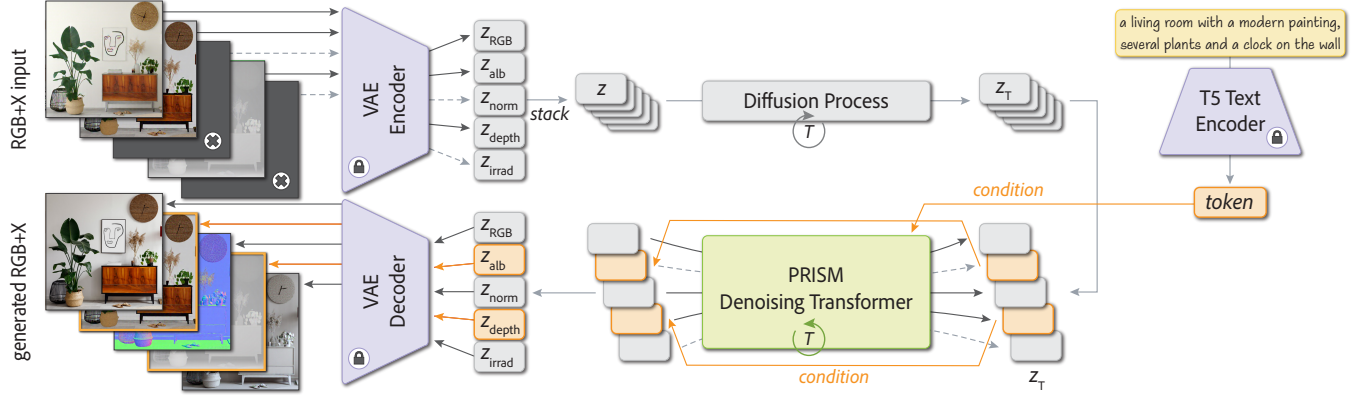


Fig. 2. **Pipeline** of our PRISM model. RGB image and its corresponding X intrinsic channels are encoded into latent space via a fixed VAE Encoder. A Diffusion Transformer is applied on the tokens of the latent of all channels simultaneously and conditioned by the text embedding from an input text prompt. Denoised tokens are passing through a fixed decoder for RGB+X generation. During training, intrinsic channels are randomly ablated which makes PRISM a unified framework for text-to-image generation, intrinsic decomposition, and conditional image generation with any subset of intrinsic images.

fundamental problem since many image editing tasks (relighting, material editing, and geometric manipulation) can be represented as specific changes in the corresponding intrinsic maps. Hence, instead of replacing the image generation capability with a perception task, we propose that generation and perception tasks should be handled in a unified manner. Such a unified framework preserves the original image generation capability of the foundational model while the generative prior can simultaneously be utilized for perception.

In this paper, we present PRISM, a unified framework that jointly addresses intrinsic image decomposition and conditional image generation. Starting from a pre-trained diffusion transformer model for image generation, PRISM presents an effective approach to fine-tune the base model to jointly generate RGB images along with its intrinsic maps (which we denote as X layers). Our model enables conditional generation with any combination of X layers while preserving text-based generation. PRISM can perform: (i) text-to-RGBX generation, where text input produces an image with intrinsic layers, (ii) RGB-to-X decomposition from an input image, and (iii) X-to-RGBX generation from a subset of intrinsic layers. Since all X layers are generated jointly, PRISM achieves an improved alignment between the RGB image and each of the intrinsic maps. The third task enables global image editing by conditioning on selected intrinsic maps and text prompts that describe the edits (e.g., for relighting, we condition generation on all the intrinsic maps except the shading layer along with a text prompt that describes the desired lighting). We additionally enable local editing through fine-tuning with masked conditioning maps.

We extensively evaluate PRISM, compare it with strong baselines, and demonstrate competitive performance on multiple tasks. Our method excels in intrinsic image decomposition and consistency across modalities, while also delivering competitive results with respect to visual and conditional generation quality. Even though we use limited datasets when training PRISM, we observe a strong generalization capability when performing RGB-to-X decomposition which we attribute to the unified generation and perception capability. Finally, we show case various downstream applications, such

as material editing and relighting, that benefit from our approach. By jointly generating images along with their intrinsic modalities, PRISM facilitates iterative editing of an image while maintaining consistent intrinsic decomposition. In summary, our main contributions include: 1) a unified multi-tasking model for both intrinsic perception and conditional generation that demonstrates strong generalization capability; 2) joint generation of intrinsic layers and RGB images for improved alignment; and 3) competitive performance in intrinsic decomposition and downstream applications.

2 RELATED WORK

2.1 Text-to-Image Generation

Text-to-image generation has seen significant advancements in recent years following earlier works on class-conditional and unconditional large-scale image generation models with GAN [Brock et al. 2018; Karras et al. 2021, 2019, 2020; Mirza and Osindero 2014; Reed et al. 2016] and diffusion-based [Dhariwal and Nichol 2021; Ho et al. 2020] architectures. Earlier works on text-to-image generation predominantly use GANs [Reed et al. 2016; Tao et al. 2022; Xia et al. 2021; Xu et al. 2018; Zhang et al. 2017; Zhu et al. 2019]. They either operate in specific domains with limited vocabularies or formulate text-to-image generation as a text-guided editing problem. While works like GigaGAN [Kang et al. 2023] demonstrate that it is possible to scale up GANs as foundational image generators, diffusion models and large-scale language encoders [Radford et al. 2021; Raffel et al. 2019] have been pre-dominantly used for text-based image generation in the recent years. Works such as GLIDE [Nichol et al. 2021], DALL-E 2 [Ramesh et al. 2022], and Imagen [Saharia et al. 2022] propose diffusion-based architectures that can generate photorealistic images from text descriptions using a pre-trained frozen text encoder [Radford et al. 2021; Raffel et al. 2019]. Following the success of U-Net based diffusion models, other variants including transformer-based auto-regressive and diffusion models [Chen et al. 2023; Ding et al. 2021, 2022; Gafni et al. 2022; Ramesh et al. 2021; Yu et al. 2022] have been widely adopted. We base our work on a pre-trained diffusion transformer-based text-to-image generation

model and fine-tune it to jointly generate images along with its intrinsic maps.

2.2 Image Editing with Diffusion Models

Several methods have been proposed to add additional conditioning to text-to-image diffusion models to enable custom generation and editing. One approach is to perform large-scale training for task-specific purposes such as domain adaptation and personalization [Gal et al. 2022; Hu et al. 2022; Ruiz et al. 2022]. Composer [Huang et al. 2023] formulates image generation as a composition problem and trains a model that takes a text prompt and optional style and content images as input to generate a final image. Kosmos [Pan et al. 2023; Peng et al. 2023], QWEN-VL [Bai et al. 2023] and OmniGen [Xiao et al. 2024] propose large scale generative vision-language models that enable image editing via leveraging the model’s linguistic reasoning capabilities. Finally, works such as InstructPix2Pix [Brooks et al. 2022] propose training a diffusion model on input image and edited image pairs with edit instructions to enable instruction-based editing.

In another line of work, methods such as ControlNet [Li et al. 2024c; Zhang et al. 2023; Zhao et al. 2023], T2I-Adapter [Mou et al. 2023b], GLIGEN [Li et al. 2023b] and IP-Adapter [Ye et al. 2023] propose training lightweight adapter modules to inject new conditioning information into the latent space of pre-trained diffusion models. They fine-tune the adapter modules while keeping original diffusion models frozen to condition the generation on various modalities such as RGB images, depth maps, skeletal pose images, face identity embeddings [Papantoniou et al. 2024], etc.

Finally, works such as Prompt2Prompt [Hertz et al. 2022], MasaCtrl [Cao et al. 2023] and DragonDiffusion [Mou et al. 2023a] propose attention-based latent manipulation methods to enable fine-grained and targeted edits of both generated and real images. Our unified PRISM framework enables conditioned image generation as well as image editing by iteratively manipulating the intrinsic channels that are either jointly generated or predicted from input images. We provide examples of both global and local editing results in Section 4.3.

2.3 Intrinsic Image Decomposition

Intrinsic image decomposition aims to decompose RGB images into appearance and geometry-related channels like albedo, irradiance, depth, and surface normals. Early approaches proposed heuristics that operate on image gradients [Land and McCann 1971], grayscale [Barron and Malik 2012; Tappen et al. 2006, 2005], or RGB images [Garces et al. 2012; Gehler et al. 2011; Liao et al. 2013; Liu et al. 2012; Zhao et al. 2012], with some leveraging additional input [Barron and Malik 2013]. These methods relied on optimization based on assumed priors about albedo, illumination, and shape properties.

With the adoption of learning based methods for various graphics and vision tasks, follow up work in intrinsic image decomposition also adopted neural networks to tackle the problem [Fan et al. 2018; Jin et al. 2023; Li and Snavely 2018a; Liu et al. 2020; Narihira et al. 2015; Zhou et al. 2015; Zoran et al. 2015] along with efforts to curate relevant dataset [Bell et al. 2014a; Li and Snavely 2018a; Li et al.

2021; Roberts et al. 2021a]. Other recent work [Careaga and Aksoy 2023, 2024] focused on illumination and divided the problem into physically-motivated sub-problems that can be modeled with neural networks. In addition to supervised training, methods were proposed that exploit multi-task learning [Kim et al. 2016; Luo et al. 2020; Zhou et al. 2019] and unsupervised learning [Lettry et al. 2018; Li and Snavely 2018b].

Recent work has adapted foundational text-to-image models for inverse tasks like depth [Ke et al. 2024] and normal estimation [Ye et al. 2024]. In a similar fashion, several methods have been proposed to explore latent directions in pre-trained models like StyleGAN [Bhattad et al. 2023] or fine-tune diffusion models [Du et al. 2023; Kocsis et al. 2024; Luo et al. 2024a; Zeng et al. 2024; Zhao et al. 2025] to generate intrinsic channels conditioned on an input image. Our work follows a similar spirit, but to the best of our knowledge, PRISM is the first unified model that can simultaneously generate RGB and intrinsic channels while also enabling conditioning with respect to any combination of the channels.

3 METHOD

3.1 Diffusion Models

Diffusion models [Dhariwal and Nichol 2021; Ho et al. 2020; Nichol et al. 2021; Peebles and Xie 2022] are a class of generative models that generate data from Gaussian noise via an iterative denoising process. Typically, a simple mean-squared diffusion loss is used as the denoising objective:

$$\mathcal{L}_{\text{simple}} = \mathbb{E}_{\mathbf{x}_0, \mathbf{c}, \epsilon, t} (\|\epsilon - \epsilon_\theta(a_t \mathbf{x}_0 + \sigma_t \epsilon, \mathbf{c})\|_2^2), \quad (1)$$

where \mathbf{x}_0 are training samples with optional conditions \mathbf{c} , $t \sim \mathcal{U}(0, 1)$ denotes the diffusion timestep, $\epsilon \sim \mathcal{N}(0, \mathbf{I})$ is the additive Gaussian noise, a_t, σ_t are scalar functions of t determined by the underlying scheduler, and ϵ_θ is a diffusion model with learnable parameters θ . *Classifier-free guidance* is most widely employed in recent works [Nichol et al. 2021; Ramesh et al. 2022; Rombach et al. 2021; Saharia et al. 2022] for conditional data sampling from a diffusion model, where the predicted noise is adjusted via:

$$\hat{\epsilon}_\theta(\mathbf{x}_t, \mathbf{c}) = \omega \epsilon_\theta(\mathbf{x}_t, \mathbf{c}) + (1 - \omega) \epsilon_\theta(\mathbf{x}_t), \quad (2)$$

where $\mathbf{x}_t = a_t \mathbf{x}_0 + \sigma_t \epsilon$, and ω is a guidance weight. Sampling algorithms such as DDIM [Song et al. 2020] and DPM-Solver [Lu et al. 2022a,b] are often adopted to speed up the sampling process of diffusion models.

3.2 PRISM

Base Model. We base our work on a pre-trained diffusion transformer architecture (DiT) [Peebles and Xie 2022] that flexibly handles both text and image conditioning through random condition token dropout during training. During training, images are first encoded into the latent space of the diffusion model and then tokenized as patches. Our denoiser architecture provides textual and image embeddings extracted via frozen text and image encoders to the attention layers in each transformer block. Specifically, it follows a standard decoder-only transformer architecture containing self-attention blocks where image and text embeddings are tokenized and appended to the tokens of the image being generated. We follow previous work [Chen et al. 2023; Esser et al. 2024; Saharia et al.

2022] to employ the T5 large language model [Raffel et al. 2019] as our text encoder. The diffusion timestep is directly added to the image tokens as positional encoding. Once a clean latent image representation is sampled, it is then decoded into the RGB image space. In our experiments, we keep the VAE frozen and only fine-tune the diffusion denoiser. While our base model is flexibly text and image conditioned, PRISM utilizes only the text conditioning, which enables robust performance even in scenarios without text inputs, such as RGB-to-X decomposition tasks.

Joint RGBX Generation. Given the pre-trained text-to-image model, PRISM extends it to generate an RGB image along with its intrinsic properties resulting in a fixed number, M , of output images. PRISM enables conditioned generation based on a combination of text prompts and a flexible number of intrinsic maps. We propose an effective fine-tuning strategy without any architectural changes as we discuss next.

Let T_{base} denote the number of input tokens the base model operates on. To accommodate generation with multiple modalities, we expand the input token size to T_{new} as:

$$T_{new} = T_{base} \times M \quad (3)$$

where M is the number of modalities ($M = 5$ in our implementation, corresponding to RGB, albedo, normal, depth, and irradiance). Specifically, we encode and patchify each intrinsic map separately and provide a union of all tokens as input to the diffusion network. This expansion enables the tokens of the different modalities to jointly attend to each other in the attention blocks of the diffusion model, and results in output RGB images and intrinsic maps to be spatially aligned. We further adjust the positional encoding of the input tokens such that the network can distinguish which token belongs to which modality. Once a clean set of tokens is generated, we group and decode the tokens of each modality independently.

We augment PRISM with a flexible conditioning mechanism that enables conditioning on both text and a variable number of intrinsic maps. Let $x_t \in \mathbb{R}^{T_{new} \times d} = \bigcup_{i=1}^M x_t^i$ represent the union of all noisy latent tokens at timestep t , where x_t^i denotes a modality, M is the total number of modalities, and d is the embedding dimension. We denote the set of conditioning modalities as: C where $0 \leq |C| \leq M$. At each diffusion step, we perform a slight modification to enable conditional generation. After each noise prediction, we override the tokens of a conditioning modality with its clean counterparts as follows:

$$x_t^i = \begin{cases} x_0^i & \text{if } i \in C \\ x_t^i & \text{otherwise} \end{cases} \quad (4)$$

These simple changes keep the conditioning modalities unchanged and ensure the remaining modalities are influenced by them. At inference time, PRISM can be utilized for three common tasks: (i) text-to-multi-modality generation by setting $C = \emptyset$, (ii) intrinsic image decomposition by conditioning on an RGB image, and (iii) conditional image generation by providing at least one of the intrinsic maps as conditions.

3.3 Implementation Details

Intrinsic channels. We train PRISM to output the following channels along with RGB images:

- Surface normal $\mathbf{n} \in \mathbb{R}^{H \times W \times 3}$ specifying per-pixel surface normal defined in the camera coordinates;
- Depth $\mathbf{d} \in \mathbb{R}^{H \times W \times 3}$ represented as per-pixel disparity in the camera coordinates. We represent the depth as a 3-channel image by replicating the disparity value along the channel dimension.
- Albedo $\mathbf{a} \in \mathbb{R}^{H \times W \times 3}$, also commonly referred to as base color, which specifies the diffuse albedo for dielectric opaque surfaces;
- Diffuse irradiance $\mathbf{e} \in \mathbb{R}^{H \times W \times 3}$, serving as a lighting representation and is defined similar to Zeng et al. [2024].

Datasets. Our approach requires a diverse dataset of paired RGB images and intrinsic channels (normal n , depth d , albedo a , diffuse irradiance e), along with text captions for training. Following previous work [Zeng et al. 2024], we combine multiple data sources to fulfill this requirement. We utilize InteriorVerse [Zhu et al. 2022], a synthetic indoor scene dataset with over 50,000 rendered images providing \mathbf{n} , \mathbf{d} , and \mathbf{a} channels. Similar to Zeng et al. [2024], to mitigate synthetic noise in this dataset, we apply denoising on the rendered images. We also use HyperSim [Roberts et al. 2021b], a photorealistic dataset of more than 70,000 rendered images with \mathbf{n} , \mathbf{d} , \mathbf{a} , and \mathbf{e} channels. To further enhance the realism and diversity of our training data, we use an internal dataset of 50,000 high-quality commercial interior images where only the RGB modality is available. To preserve the text-understanding capabilities of our model, we generate captions for all images in the combined dataset using BLIP-2 [Li et al. 2023a].

Training Strategy. As we train PRISM on datasets with varying modalities available, we adopt several strategies to facilitate training. First, if a modality is not provided in a given dataset, we use zero-padded placeholder images, $x_t^m = 0$, where m denotes a missing modality. We exclude these missing modalities from the corresponding loss computation. For each batch, we randomly select a subset of available modalities as conditioning signals to effectively perform multi-task training including text-only generation, intrinsic decomposition, and conditional generation. Finally, we implement data source-consistent batching and stratified sampling to maintain identical percentages of each data source between training and validation sets. This balanced representation of modality combinations and conditioning scenarios improves training stability, given varying modality availability across sources.

Inference Settings. We use PRISM in three main modes including text-to-RGBX generation, RGB-to-X intrinsic decomposition, and X-to-RGBX conditional image generation. For intrinsic decomposition, since we are mostly interested in predicting intrinsic maps of a given RGB image, we find it unnecessary to provide an additional text prompt as input. Hence, in this mode we also disable CFG by setting the guidance weight $\omega = 0$. In other modes, we set the guidance weight $\omega = 7.5$.

Inpainting. Various image editing tasks focus on locally editing a region, e.g., changing the appearance properties of a particular object as shown in Figure 7. To support such cases, we fine-tune PRISM model to support inpainting, i.e., conditioning with masked input maps. Specifically, during training, we simply introduce random masks [Suvorov et al. 2021] in conditioning maps where we

set the latent condition map inside the mask region to be random gaussian noise. When computing the diffusion loss, we discard any masked area in the different maps to enable the network to learn to *inpaint* such regions.

4 EXPERIMENTS

We perform qualitative and quantitative experiments to showcase the capabilities of PRISM for intrinsic image decomposition, joint image generation, conditional image generation, and editing.

4.1 Implementation Details

Training and Evaluation Details. We fine-tune our base text-to-image model on InteriorVerse [Zhu et al. 2022], HyperSim [Roberts et al. 2021b] datasets, and an internal commercial dataset consisting of real images of interior scenes. We train our model with a batch size of 128 using the AdamW optimizer [Loshchilov and Hutter 2017] with a weight decay of 0.1 and a constant 5×10^{-5} learning rate, and fine-tune for 15,000 steps on 8 A100 GPUs. We perform aspect ratio-preserving resizing and random crop of 512×512 for training and avoid using a random horizontal flip since it disrupts the camera-space normals. The training of our PRISM model takes around 30 hours and the fine-tuning to enable inpainting takes around 10 hours on 8 A100 GPUs.

For all experiments, we use the official code bases of baseline methods with default settings or use their self-reported metrics where applicable. For conditional image generation experiments, we test our method on the validation set of the pseudo-labeled ImageNet dataset released by Li et al. [2024b]. For consistency with the baseline conditional image generation methods, we downsample our generated results to 256×256 resolution to compute FID scores. For all conditional image generation baselines, we report their self-reported metrics. For intrinsic image decomposition experiments, we use the official code bases of all baseline methods and run their methods with their respective default settings. For Table 1, we directly utilize the baseline metrics provided in Zeng et al. [2024] on the HyperSim test set and run our method on the same test set. For evaluations on the InteriorVerse dataset, we use our custom train-test split as InteriorVerse does not have a designated test set.

Baselines. We compare our method with state-of-the-art conditional generation and intrinsic image decomposition methods. More specifically, for intrinsic decomposition, we compare against the recent diffusion based [Kocsis et al. 2024; Zeng et al. 2024] and non-diffusion based [Careaga and Aksoy 2023, 2024] methods. We additionally consider an internal method, PVT-normal, based on Pyramid Vision Transformer [Wang et al. 2022] and trained on datasets similar to MiDaS [Birkel et al. 2023; Ranftl et al. 2022] to estimate normals. For conditional generation, we compare with ControlNet [Zhang et al. 2023], T2I-Adapter [Mou et al. 2023b], ControlVAR [Li et al. 2024b] and CAR [Yao et al. 2024]. For depth estimation, we compare our method to a number of state-of-the-art monocular relative and metric depth estimation methods, including Marigold [Ke et al. 2024] and Depth Anything [Yang et al. 2024a,b]. Where applicable, we report self-reported metrics of additional baselines for which the codebase or pretrained models are not available.

Table 1. Quantitative evaluation of PRISM’s intrinsic image decomposition performance against baseline methods on HyperSim test set.

Method	Albedo		Normal		Irradiance	
	PSNR \uparrow	LPIPS \downarrow	PSNR \uparrow	LPIPS \downarrow	PSNR \uparrow	LPIPS \downarrow
PRISM (ours)	19.3	0.18	19.9	0.18	18.5	0.20
Zeng et al. [2024]	17.4	0.18	19.8	0.18	14.1	0.22
Zhu et al. [2022]	11.7	0.54	16.5	0.45	-	-
Careaga and Aksoy [2023]	13.5	0.34	-	-	-	-
Kocsis et al. [2024]	12.1	0.41	-	-	-	-
PVT-normal	-	-	18.8	0.30	-	-
PRISM-albedo	18.4	0.19	-	-	-	-
PRISM-normal	-	-	18.9	0.19	-	-
PRISM-irradiance	-	-	-	-	17.9	0.21

Evaluation Metrics. We report Inception Score (IS) [Salimans et al. 2016] and Frechet Inception Distance (FID) [Heusel et al. 2017] to assess the quality of generated RGB images and additionally utilize the CLIP Score [Hessel et al. 2021] to assess the adherence of generated images to the input text prompts. For intrinsic image decomposition, we report the mean PSNR [Zhang et al. 2018a] and LPIPS [Zhang et al. 2018b] metrics between the ground truth and generated albedo, normal, and irradiance on the HyperSim test set. To evaluate the depth estimation quality of our method, we report Absolute Relative Error (AbsRel) and Threshold Accuracy (δ_1) metrics on the NYU-v2 [Silberman et al. 2012] and ETH3D [Schöps et al. 2017] datasets. As PRISM is trained to estimate disparity, we first convert our estimated disparity maps to relative depth maps.

Qualitative results. We start by showcasing the capabilities of our model for various tasks in Figure 3 including text-based joint generation (text-to-RGBX), intrinsic image decomposition (RGB-to-X), conditional generation (X-to-RGBX). As shown, our model can generate realistic and diverse results even in pure text-conditioned cases and adapts to different input condition settings.

4.2 Quantitative Evaluation

Intrinsic image decomposition. We show visual intrinsic image decomposition results for synthetic samples in Figure 4 along with various baseline outputs. For all experiments, we generate 5000 samples and provide quantitative metrics in Table 1 where we report the numbers for baseline methods whenever applicable. PRISM performs on-par or superior to state-of-the-art methods while being a unified model capable of multiple tasks.

In order to assess the benefit of jointly estimating multiple modalities on the accuracy of predicting individual maps, we train multiple single image output variants of our method to solely predict albedo, normals, and irradiance given an input RGB image. As shown in Table 1, PRISM consistently performs better than its uni-modal variants across all modalities, demonstrating the advantage of joint prediction.

We also evaluate PRISM and the baseline intrinsic decomposition methods on the InteriorVerse test set and report the results in Table 2. Our method demonstrates superior performance which is consistent to the results shown in Table 1.

We separately evaluate the depth estimation quality of our method against a number of state-of-the-art monocular relative and metric depth estimation methods on the NYU-v2 [Silberman et al. 2012] and ETH3D [Schöps et al. 2017] datasets. As shown in 7, our method

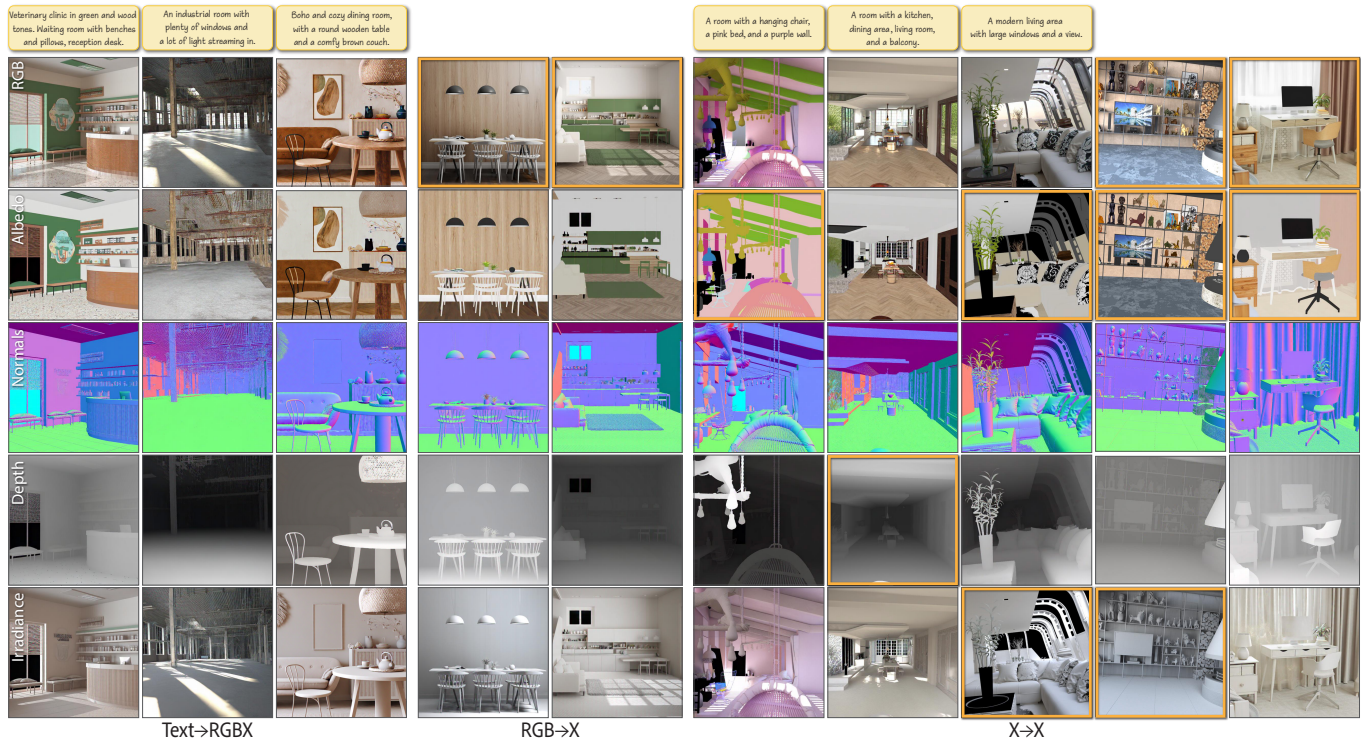


Fig. 3. Sample results generated with PRISM. Our model is capable of text, text+X and X conditioned generation and can inherently perform image decomposition and re-composition under different material, geometry and lighting conditions. Condition channels are highlighted in orange.

Table 2. Quantitative evaluation of PRISM’s intrinsic image decomposition performance on InteriorVerse test set.

Method	Albedo		Normal	
	PSNR↑	LPIPS↓	PSNR↑	LPIPS↓
PRISM (ours)	19.9	0.14	21.2	0.15
Zeng et al. [2024]	16.6	0.17	20.2	0.19
Zhu et al. [2022]	13.6	0.24	17.1	0.26
Careaga and Aksoy [2023]	17.4	0.20	-	-
CID	17.7	0.27	-	-
Kocsis et al. [2024]	12.2	0.30	20.1	0.21
PRISM-albedo	18.9	0.15	-	-
PRISM-normal	-	-	20.4	0.16
PVT-normal	-	-	17.4	0.25

achieves competitive results despite having been trained on a much smaller and solely indoor dataset.

Furthermore, a common issue when processing individual intrinsic maps separately is the alignment across different modalities, e.g., the white balance ambiguity between albedo and irradiance. Here, we report reconstruction error of PRISM, PRISM single channel variant where we use PRISM-albedo and PRISM-irradiance to estimate albedo and irradiance separately, as well as the strongest baseline [Zeng et al. \[2024\]](#). Specifically, given an RGB image and the corresponding maps, we reconstruct the diffuse appearance of

the target image simply by multiplying albedo and irradiance maps. We then compare the reconstructed image of the two approaches to the ground truth. The brightness of the reconstructed image will be shifted if the two channels are not aligned in terms of white balance. We show the metrics of the two approaches on the HyperSim test set in Table 3, as well as some visual examples in Figure 5. Our method generates reconstructions closer to the ground truth which we attribute to the fact that jointly generating multiple modalities result in intrinsic channels that are better aligned. We also note that PRISM single channel leads to degradation in performance compared to our final PRISM model, which shows the advantage of joint generation over single channel estimation.

Table 3. We report the reconstruction error for PRISM, PRISM single channel variant and Zeng et al. [2024]. The reconstruction is conducted by multiplying the predicted albedo and irradiance. Our joint inference strategy addresses the white balance ambiguity between albedo and irradiance, leading to improved quantitative and qualitative performance.

Input	RMSE ↓	PSNR ↑	LPIPS ↓
PRISM	0.0849	22.38	0.15
PRISM single channel	0.1299	19.94	0.16
Zeng et al. [2024]	0.1437	16.55	0.16

We further evaluate our method on the out-of-domain synthetic ARAP dataset [Bonnee et al. 2017] following the same experimental setup as CID [Careaga and Aksoy 2024] and report the results in

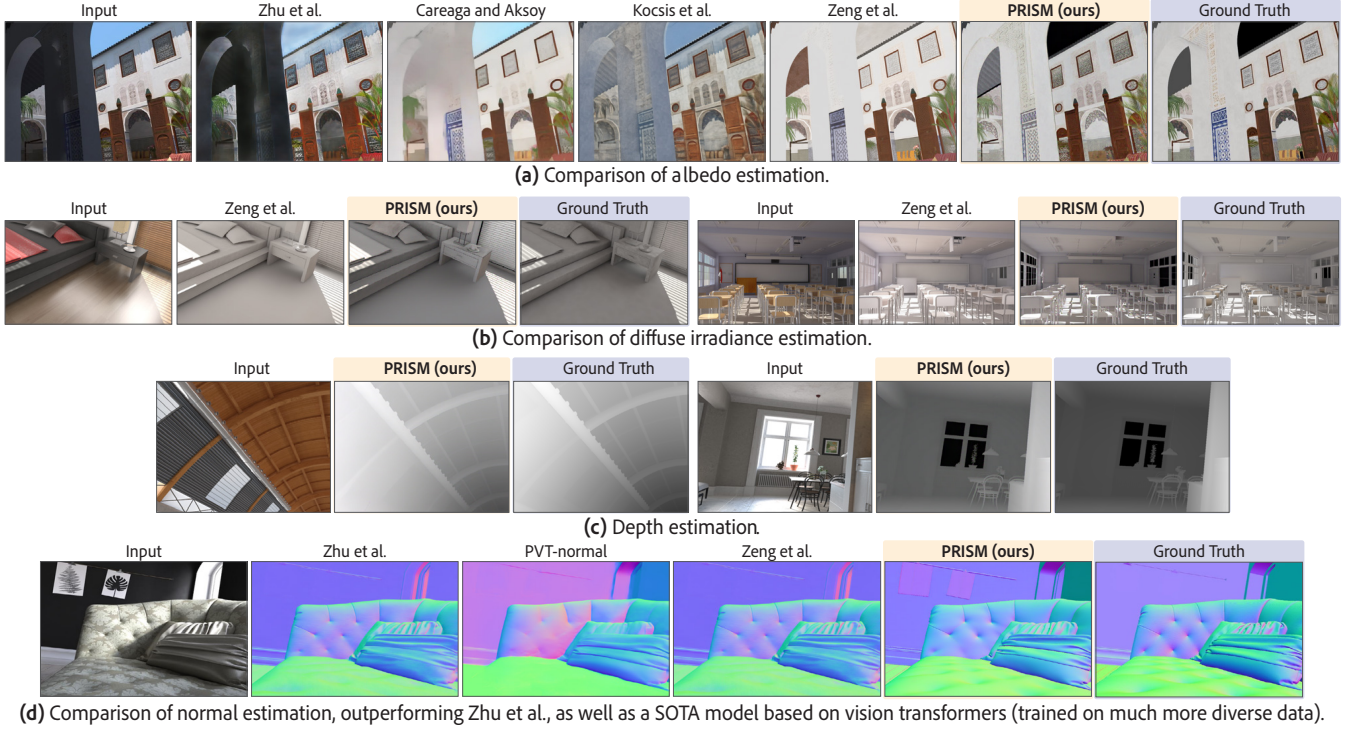


Fig. 4. Visual comparison of our PRISM model against baseline methods on synthetic datasets. All input images and ground truths are from the HyperSim dataset, except for the classroom scene (b, right).



Fig. 5. Visual comparison of RGB reconstruction from predicted albedo and irradiance for the white balance alignment. We compare PRISM model against Zeng et al. [2024] and ground truth reconstructions.

Table 4. As shown in Table 4, our method is on-par with the SOTA method CID and better than previous diffusion-based methods.

In addition to evaluations on synthetic test sets, we evaluate our method on two real datasets with respect to albedo estimation quality: IIW [Bell et al. 2014b] and MAW [Wu et al. 2023] datasets. We first evaluate our method on the Intrinsic Images in-the-Wild (IIW) dataset, which provides pairwise human annotations of albedo brightness between sparsely sampled pixels, and present the results in Table 5. Although our method is outperformed by Careaga and Aksoy [2024] by a close margin, we note that the transparent surfaces in the IIW dataset are marked as white, while some of our

Table 4. Zero-shot albedo evaluation on the synthetic ARAP Dataset [Bon-neel et al. 2017]. Our proposed method estimates is on-par with SOTA CID method, and outperforms it in terms of SSIM.

Method	LMSE ↓	RMSE ↓	SSIM ↑
Chromaticity	0.038	0.193	0.710
Constant Shading	0.047	0.264	0.693
Luo et al. [2023] *	0.023	0.129	0.788
Kocsis et al. [2024]	0.030	0.160	0.738
Zhu et al. [2022]	0.029	0.184	0.729
Careaga and Aksoy [2023]	0.035	0.162	0.751
Careaga and Aksoy [2024]	0.021	0.149	0.796
PRISM	0.022	0.149	0.798

datasets treat them as black, which we think leads to some discrepancy. For the MAW dataset, which consists of ~850 indoor images and measured albedo within specific masked regions in the image, we report the intensity and chromaticity of albedo estimates in Table 6.

Joint image generation. We evaluate the text-to-image generation performance of PRISM against our base text-to-image model using FID and text/image CLIP similarity scores in Table 8. To this end, we generate 5000 samples using the same text prompts both from our base model and PRISM. We use the MJHQ-30k [Li et al. 2024a] dataset as the reference real images. We curate the testing text prompts from the MJHQ-30k and the testing split of the Hypersim dataset. We notice that PRISM exhibits a slight degradation

Table 5. We report the WHDR error of albedo estimates on the IIW dataset for PRISM and baselines.

Method	WHDR 10%↓	WHDR 20%↓
Zhu et al. [2022]	34.7	24.1
Careaga and Aksoy [2023]	24.8	19.2
Luo et al. [2023]	12.8	10.8
Luo et al. [2024b]	17.9	13.3
Kocsis et al. [2024]	26.1	20.7
Zeng et al. [2024]	23.6	21.1
Careaga and Aksoy [2024]	16.8	15.6
PRISM	17.2	15.9

Table 6. We report the intensity and chromaticity of albedo estimates on the MAW dataset for PRISM and baselines.

Method	Intensity (x100)↓	Chromaticity↓
Zhu et al. [2022]	1.44	4.94
Careaga and Aksoy [2023]	0.57	6.56
Kocsis et al. [2024]	1.13	5.35
Zeng et al. [2024]	0.82	3.96
Chen et al. [2024]	0.98	4.12
Careaga and Aksoy [2024]	0.54	3.37
PRISM	0.71	3.92

Table 7. Zero-shot relative depth estimation. Better: AbsRel ↓, δ_1 ↑. Our method achieves depth estimation results comparable to current SOTA methods despite having been trained on a fraction of the data.

Method	NYU-v2		ETH3D	
	AbsRel ↓	δ_1 ↑	AbsRel ↓	δ_1 ↑
DiverseDepth [Yin et al. 2021]	0.117	0.875	0.228	0.694
MiDaS [Ranftl et al. 2019]	0.111	0.885	0.184	0.752
LeReS [Yin et al. 2020]	0.090	0.916	0.171	0.777
Omidata [Eftekhar et al. 2021]	0.074	0.945	0.166	0.778
DPT [Ranftl et al. 2021]	0.098	0.903	0.078	0.946
HDN [Zhang et al. 2022]	0.069	0.948	0.121	0.833
Depth Anything V1 [Yang et al. 2024a]	0.043	0.981	0.127	0.882
Depth Anything V2 [Yang et al. 2024b]	0.045	0.979	0.131	0.865
Marigold [Ke et al. 2024]	0.055	0.964	0.065	0.960
PRISM	0.061	0.922	0.142	0.836

in performance which can be attributed to the fact that it has been mostly trained on synthetic indoor images. Hence, we also use the interior subset of MJHQ-30k-interior that consists of mostly indoor scenes as the real reference set for computing FID. In this case PRISM performs slightly better than the base model. Overall, we conclude that the unified generation strategy does not degrade the image generation capabilities of the base model.

Conditional image generation. Finally, we evaluate the conditional image generation performance of our model against commonly used conditioning baselines in Table 9. In addition to popular approaches like ControlNet and T2I-Adapter, we also compare against recent methods, ControlVAR [Li et al. 2024b] and CAR [Yao et al. 2024] that also use a diffusion transformer architecture. All the baselines are trained on the same ImageNet training dataset released with ControlVAR, which is pseudo-labeled with depth and surface normals predictions. At test time, we use the provided validation

split. While baselines utilize the pseudo-ground truth depth and normals provided by the dataset for conditioning, for our method we first perform intrinsic decomposition on the RGB images and use the predicted depth and normal estimates in a second pass of conditional generation. We note that our model is trained with the synthetic datasets and is tasked to generalize to the ImageNet dataset that is unseen during training in the context of this experiment. As shown in Table 9, our model is on-par or superior to all the baselines in terms of the FID and IS metrics. We argue that our model’s joint and aligned image generation capabilities greatly benefit controllable generation use cases.

Table 8. We evaluate the text-to-image generation performance of PRISM against our base text-to-image mode in terms of image quality assessment.

Method	Ref. Dataset	FID ↓	CLIP Score ↑
PRISM-Base	MJHQ-30k	19.39	22.80 ± 4.01
PRISM	MJHQ-30k	23.98	22.30 ± 4.79
PRISM-Base	MJHQ-interior	19.01	22.95 ± 4.02
PRISM	MJHQ-interior	14.98	23.00 ± 4.65
PRISM-Base	HyperSim	28.33	22.70 ± 4.05

4.3 Applications

PRISM enables various global and local image editing applications through a two-step process, leveraging both its decomposition and generation capabilities. In Figure 6, we demonstrate text guided relighting results. Given a source RGB image (top row), we first decompose it into its intrinsic components. Then, using all the decomposed intrinsic maps except the irradiance map, we perform conditional generation using a text prompt describing a new, desired light condition. As shown in the figure, our method generates re-lit images that consistently reflect the new lighting conditions including soft shadows, specular highlights, and indirect illumination. The relit images preserve the geometric and material properties of the original scenes while generating plausible editing results.

In Figure 7, we demonstrate local appearance editing results. We decompose a given input image into its intrinsic maps. We then selectively mask albedo and normal maps with random gaussian noise in the corresponding latent embedding. Using the masked maps as well as the unmasked depth and irradiance maps as a condition, we generate new images using an edited text prompt describing the desired appearance properties. The generated results preserve the identity of the scene in the unmasked regions as well as generating new looks for the masked objects while keeping the lighting consistent.

4.4 Qualitative Results

In Figure 9, we show more visual results from PRISM. For conditioning, we use samples from the test set of the Interior Verse dataset. We further show intrinsic image decomposition samples on real images in Figure 8 and Figure 10, and text-to-RGBX samples in Figure 11.

Table 9. Comparison with existing controllable generation approaches on ImageNet. Our PRISM surpasses baselines with respect to FID scores despite not having seen ImageNet images during training.

Methods	Depth Map		Normal Map	
	FID ↓	IS ↑	FID ↓	IS ↑
T2I-Adapter	9.9	133.6	9.5	142.8
ControlNet	9.2	150.3	8.9	155.3
ControlVAR	6.5	178.5	6.8	187.7
CAR	6.9	178.6	6.6	175.9
PRISM	5.9	159.5	5.3	165.1

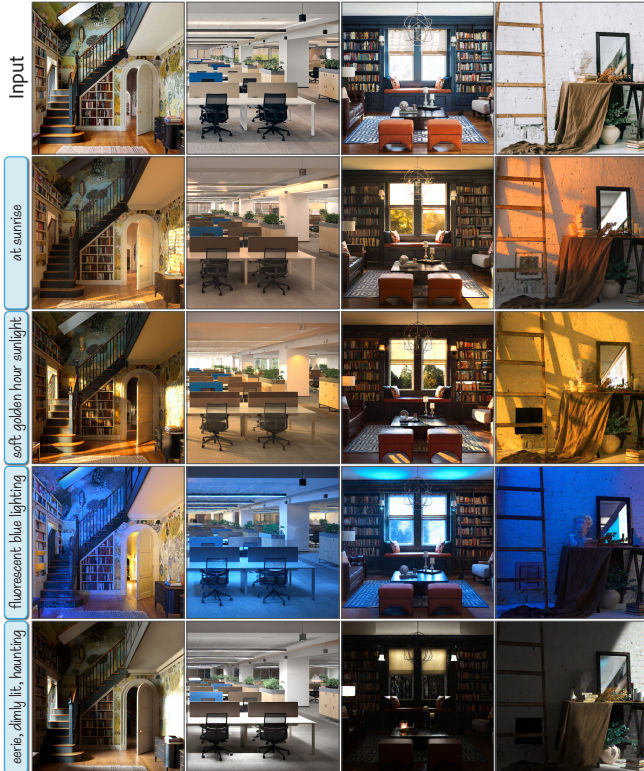


Fig. 6. **Relighting with text prompt.** Starting from an input RGB image, intrinsic layers are predicted using PRISM. We then apply PRISM with a text prompt describing a new light condition together with all predicted intrinsic layers except irradiance map. Our relit results preserve the geometric and material properties of the original scenes while achieving plausible appearance under desired lighting conditions.

5 CONCLUSION

PRISM presents a significant advancement in intrinsic image decomposition and conditional image generation, offering a unified framework that addresses key limitations of previous approaches. By generating intrinsic maps alongside RGB images within a single model, PRISM improves consistency across modalities and supports flexible, context-driven image editing tasks, including global and local adjustments. One limitation of PRISM is that it is mostly trained

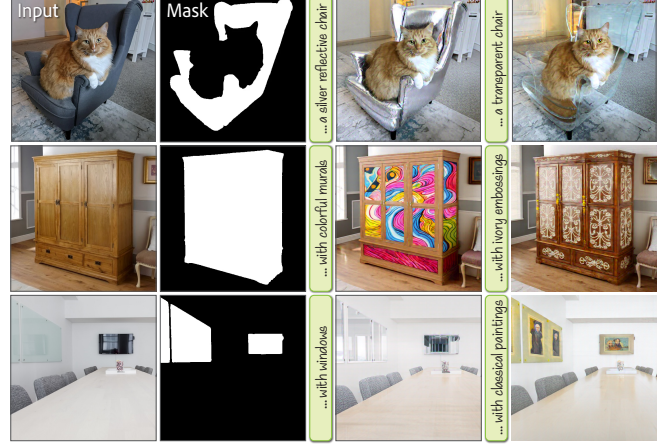


Fig. 7. **Material editing.** PRISM allows text conditioned material editing for a masked region of the input image. While keeping the predicted depth and irradiance fixed, albedo and normal channels are only conditioned outside the mask to allow the changes in the selected region conditioned by text prompt. Our results preserve the identity outside the mask while updating the appearance inside the mask with consistent lighting.

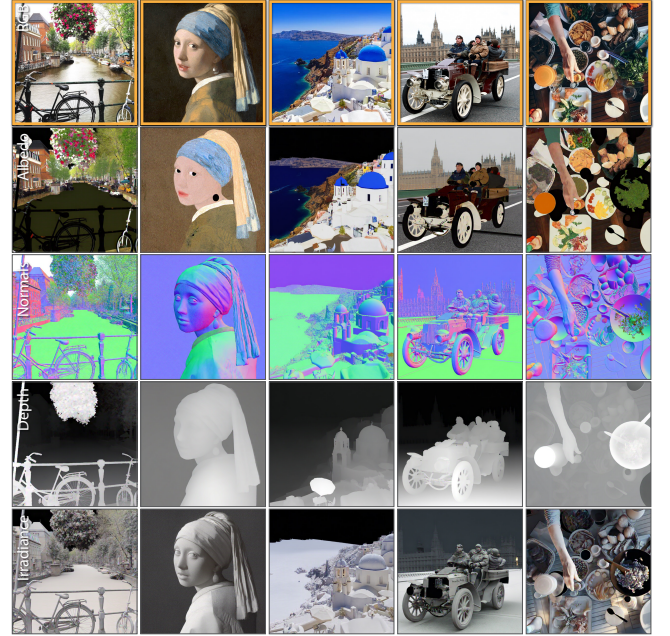


Fig. 8. **Out of Domain Examples.** Our fine-tune preserves the generalization of the base model. Here we show PRISM's intrinsic decomposition on out-of-domain cases such as outdoor, portrait, landscape, and top-down photography.

on interior scenes due to the availability of data with ground truth annotations. It is a promising future direction to use bootstrapping strategies where we use PRISM to annotate additional data samples for iterative training. Another future work is to explore additional

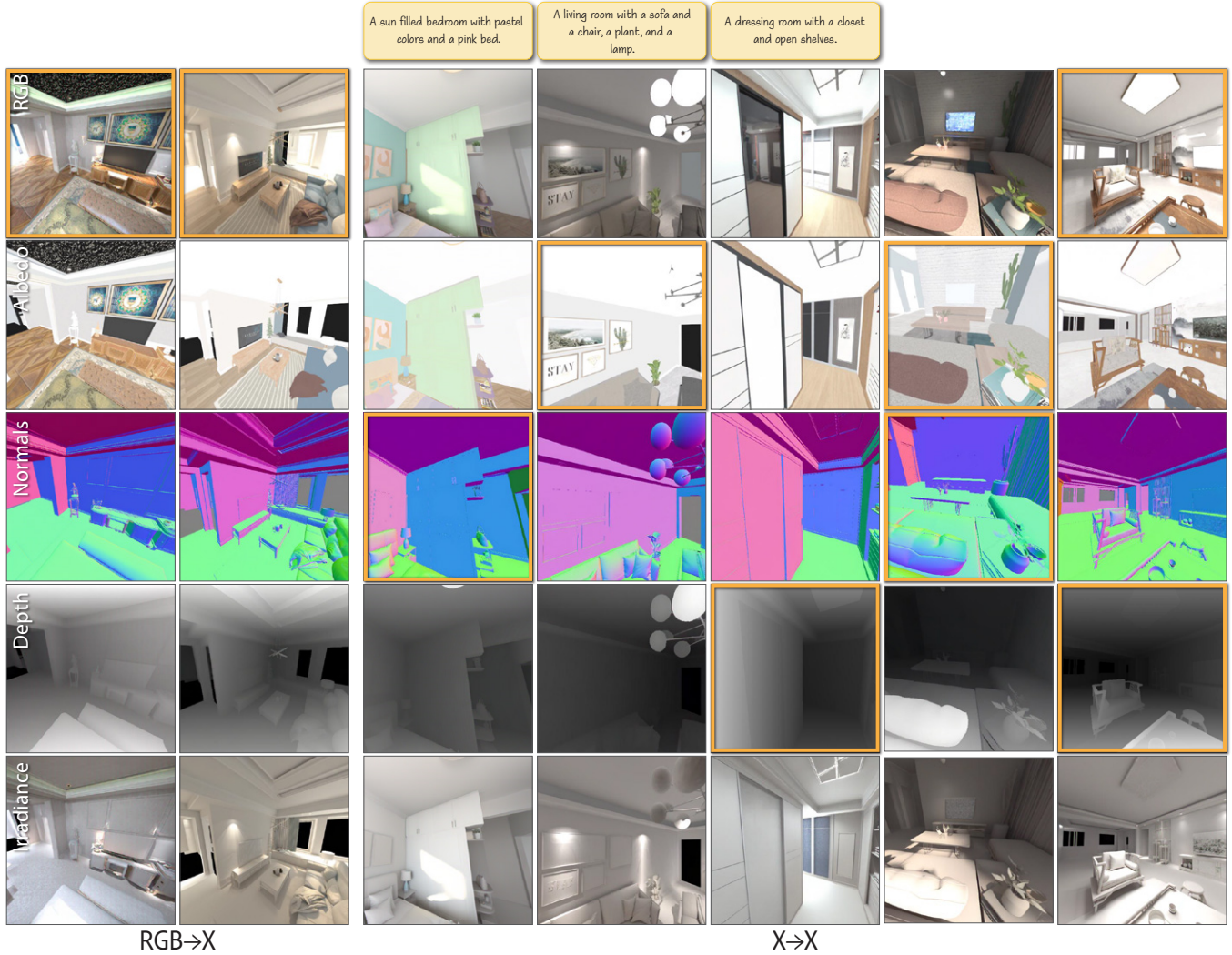


Fig. 9. Sample RGB, text+X, X+RGB conditioned results generated with PRISM on the InteriorVerse test set. Condition channels are highlighted in orange.

modalities (e.g., segmentation masks) that are synergistic with intrinsic decomposition and can aid image editing. Finally, while we simply use updated text descriptions in a standard diffusion pass to denote desired edits, exploring how targeted generative editing paradigms such as Prompt-to-Prompt [Hertz et al. 2022] and InstructPix2Pix [Brooks et al. 2022] can be built on top of PRISM is an interesting avenue.

REFERENCES

- Junze Bai, Shuai Bai, Shusheng Yang, Shijie Wang, Sinan Tan, Peng Wang, Junyang Lin, Chang Zhou, and Jingren Zhou. 2023. Qwen-VL: A Frontier Large Vision-Language Model with Versatile Abilities. *arXiv preprint arXiv:2308.12966* (2023). <https://api.semanticscholar.org/CorpusID:263875678>
- Jonathan T. Barron and Jitendra Malik. 2012. Shape, albedo, and illumination from a single image of an unknown object. *Proceedings of the IEEE/CVF International Conference on Computer Vision (ICCV)* (2012), 334–341. <https://api.semanticscholar.org/CorpusID:1342950>
- Jonathan T. Barron and Jitendra Malik. 2013. Intrinsic Scene Properties from a Single RGB-D Image. *Proceedings of the IEEE/CVF International Conference on Computer Vision (ICCV)* (2013), 17–24. <https://api.semanticscholar.org/CorpusID:7274412>
- Sean Bell, Kavita Bala, and Noah Snavely. 2014a. Intrinsic images in the wild. *ACM Transactions on Graphics (ToG)* 33, 4 (2014), 159:1–12.
- Sean Bell, Kavita Bala, and Noah Snavely. 2014b. Intrinsic images in the wild. *ACM Transactions on Graphics (TOG)* 33 (2014), 1 – 12. <https://api.semanticscholar.org/CorpusID:495068>
- Anand Bhattad, Daniel McKee, Derek Hoiem, and David Alexander Forsyth. 2023. StyleGAN knows Normal, Depth, Albedo, and More. *arXiv preprint arXiv:2306.00987* (2023). <https://api.semanticscholar.org/CorpusID:52889459>
- Reiner Birkel, Diana Wofk, and Matthias Müller. 2023. MiDaS v3.1 – A Model Zoo for Robust Monocular Relative Depth Estimation. *arXiv preprint arXiv:2307.14460* (2023).
- Nicolas Bonneel, Balazs Kovacs, Sylvain Paris, and Kavita Bala. 2017. Intrinsic Decompositions for Image Editing. *Computer Graphics Forum (Eurographics State of The Art Report)* (2017).
- Andrew Brock, Jeff Donahue, and Karen Simonyan. 2018. Large Scale GAN Training for High Fidelity Natural Image Synthesis. *arXiv preprint arXiv:1809.11096* (2018). <https://api.semanticscholar.org/CorpusID:52889459>
- Tim Brooks, Aleksander Holynski, and Alexei A. Efros. 2022. InstructPix2Pix: Learning to Follow Image Editing Instructions. *Proceedings of the IEEE/CVF Conference on Computer Vision and Pattern Recognition (CVPR)* (2022), 18392–18402. <https://api.semanticscholar.org/CorpusID:253581213>

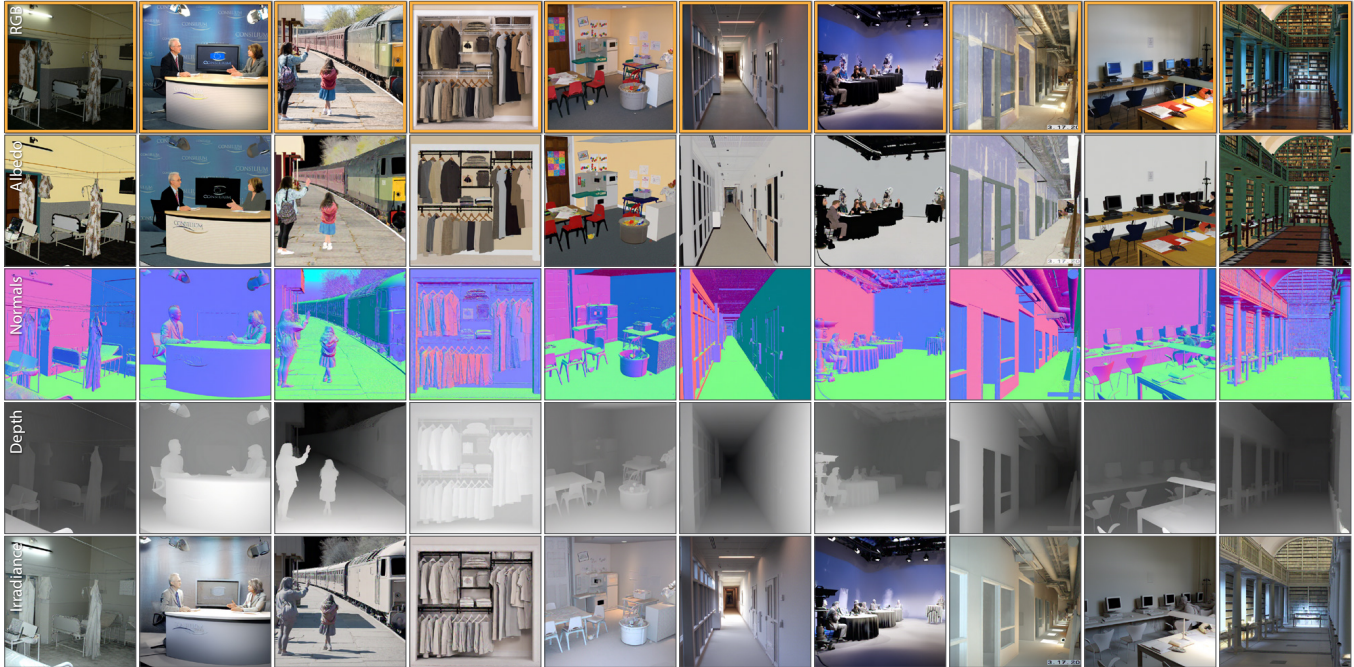


Fig. 10. Additional out of domain RGB conditioned generation samples on various indoor and outdoor images. Condition channels are highlighted in orange.

- Ming Cao, Xintao Wang, Zhongang Qi, Ying Shan, Xiaohu Qie, and Yinqiang Zheng. 2023. MasaCtrl: Tuning-Free Mutual Self-Attention Control for Consistent Image Synthesis and Editing. *Proceedings of the IEEE/CVF International Conference on Computer Vision (ICCV)* (2023), 22503–22513. <https://api.semanticscholar.org/CorpusID:258179432>
- Chris Careaga and Yağız Aksoy. 2023. Intrinsic Image Decomposition via Ordinal Shading. *ACM Transactions on Graphics (ToG)* (2023).
- Chris Careaga and Yağız Aksoy. 2024. Colorful Diffuse Intrinsic Image Decomposition in the Wild. *ArXiv abs/2409.13690* (2024). <https://api.semanticscholar.org/CorpusID:272770308>
- Junsong Chen, Jincheng Yu, Chongjian Ge, Lewei Yao, Enze Xie, Yue Wu, Zhongdao Wang, James T. Kwok, Ping Luo, Huchuan Lu, and Zhenguo Li. 2023. PixArt- α : Fast Training of Diffusion Transformer for Photorealistic Text-to-Image Synthesis. *arXiv preprint arXiv:2310.00426* (2023). <https://api.semanticscholar.org/CorpusID:263334265>
- Prafulla Dhariwal and Alex Nichol. 2021. Diffusion Models Beat GANs on Image Synthesis. *arXiv preprint arXiv:2105.05233* (2021).
- Ming Ding, Zhuoyi Yang, Wenyi Hong, Wendi Zheng, Chang Zhou, Da Yin, Junyang Lin, Xu Zou, Zhou Shao, Hongxia Yang, et al. 2021. CogView: Mastering text-to-image generation via transformers. In *Advances in Neural Information Processing Systems (NeurIPS)*.
- Ming Ding, Wendi Zheng, Wenyi Hong, and Jie Tang. 2022. CogView2: Faster and Better Text-to-Image Generation via Hierarchical Transformers. *arXiv preprint arXiv:2204.14217* (2022).
- Xiaodan Du, Nicholas I. Kolkin, Greg Shakhnarovich, and Anand Bhattad. 2023. Intrinsic LoRA: A Generalist Approach for Discovering Knowledge in Generative Models. *arXiv preprint arXiv:2311.17137* (2023).
- Ainaz Eftekhari, Alexander Sax, Jitendra Malik, and Amir Zamir. 2021. Omnidata: A Scalable Pipeline for Making Multi-Task Mid-Level Vision Datasets From 3D Scans. In *Proceedings of the IEEE/CVF International Conference on Computer Vision*. 10786–10796.
- Patrick Esser, Sumith Kulal, A. Blattmann, Rahim Entezari, Jonas Muller, Harry Saini, Yam Levi, Dominik Lorenz, Axel Sauer, Frederic Boesel, Dustin Podell, Tim Dockhorn, Zion English, Kyle Lacey, Alex Goodwin, Yannik Marek, and Robin Rombach. 2024. Scaling Rectified Flow Transformers for High-Resolution Image Synthesis. *arXiv preprint arXiv:2403.03206* (2024). <https://api.semanticscholar.org/CorpusID:268247980>
- Qingnan Fan, Jiaolong Yang, Gang Hua, Baoquan Chen, and David Wipf. 2018. Revisiting deep intrinsic image decompositions. In *Proceedings of the IEEE/CVF Conference on Computer Vision and Pattern Recognition (CVPR)*. 8944–8952.
- Oran Gafni, Adam Polyak, Oron Ashual, Shelly Sheynin, Devi Parikh, and Yaniv Taigman. 2022. Make-A-Scene: Scene-Based Text-to-Image Generation with Human Priors. In *Proceedings of the European Conference on Computer Vision (ECCV)*.
- Rinon Gal, Yuval Alaluf, Yuval Atzmon, Or Patashnik, Amit H. Bermano, Gal Chechik, and Daniel Cohen-Or. 2022. An Image is Worth One Word: Personalizing Text-to-Image Generation using Textual Inversion. *arXiv preprint arXiv:2208.01618* (2022). <https://api.semanticscholar.org/CorpusID:251253049>
- Elena Garces, Adolfo Muñoz, Jorge López-Moreno, and Diego Gutierrez. 2012. Intrinsic Images by Clustering. *Computer Graphics Forum* 31 (2012). <https://api.semanticscholar.org/CorpusID:26617945>
- Peter Gehrer, Carsten Rother, Martin Kiefel, Lumin Zhang, and Bernhard Scholkopf. 2011. Recovering Intrinsic Images with a Global Sparsity Prior on Reflectance. In *Advances in Neural Information Processing Systems (NeurIPS)*. <https://api.semanticscholar.org/CorpusID:6835647>
- Amir Hertz, Ron Mokady, Jay M. Tenenbaum, Kfir Aberman, Yael Pritch, and Daniel Cohen-Or. 2022. Prompt-to-Prompt Image Editing with Cross Attention Control. *arXiv preprint arXiv:2208.01626* (2022). <https://api.semanticscholar.org/CorpusID:251252882>
- Jack Hessel, Ari Holtzman, Maxwell Forbes, Ronan Le Bras, and Yejin Choi. 2021. CLIPScore: A Reference-free Evaluation Metric for Image Captioning. *arXiv preprint arXiv:2104.08718* (2021). <https://api.semanticscholar.org/CorpusID:233296711>
- Martin Heusel, Hubert Ramsauer, Thomas Unterthiner, Bernhard Nessler, and Sepp Hochreiter. 2017. GANs Trained by a Two Time-Scale Update Rule Converge to a Local Nash Equilibrium. In *Advances in Neural Information Processing Systems (NeurIPS)*. <https://api.semanticscholar.org/CorpusID:326772>
- Jonathan Ho, Ajay Jain, and P. Abbeel. 2020. Denoising Diffusion Probabilistic Models. *arXiv preprint arXiv:2006.11239* (2020).
- Edward J Hu, Yelong Shen, Phillip Wallis, Zeyuan Allen-Zhu, Yuanzhi Li, Shean Wang, Lu Wang, and Weizhu Chen. 2022. LoRA: Low-Rank Adaptation of Large Language Models. In *International Conference on Learning Representations (ICLR)*.
- Lianghua Huang, Di Chen, Yu Liu, Yujun Shen, Deli Zhao, and Jingren Zhou. 2023. Composer: Creative and Controllable Image Synthesis with Composable Conditions. In *Proceedings of the International Conference on Machine Learning (ICML)*. <https://api.semanticscholar.org/CorpusID:257038979>
- Yeying Jin, Ruoteng Li, Wenhan Yang, and Robby T Tan. 2023. Estimating Reflectance Layer from A Single Image: Integrating Reflectance Guidance and Shadow/Specular Aware Learning. In *Proceedings of the AAAI Conference on Artificial Intelligence*.
- Minguk Kang, Jun-Yan Zhu, Richard Zhang, Jaesik Park, Eli Shechtman, Sylvain Paris, and Taesung Park. 2023. Scaling up GANs for Text-to-Image Synthesis. *Proceedings of the IEEE/CVF Conference on Computer Vision and Pattern Recognition (CVPR)* (2023).

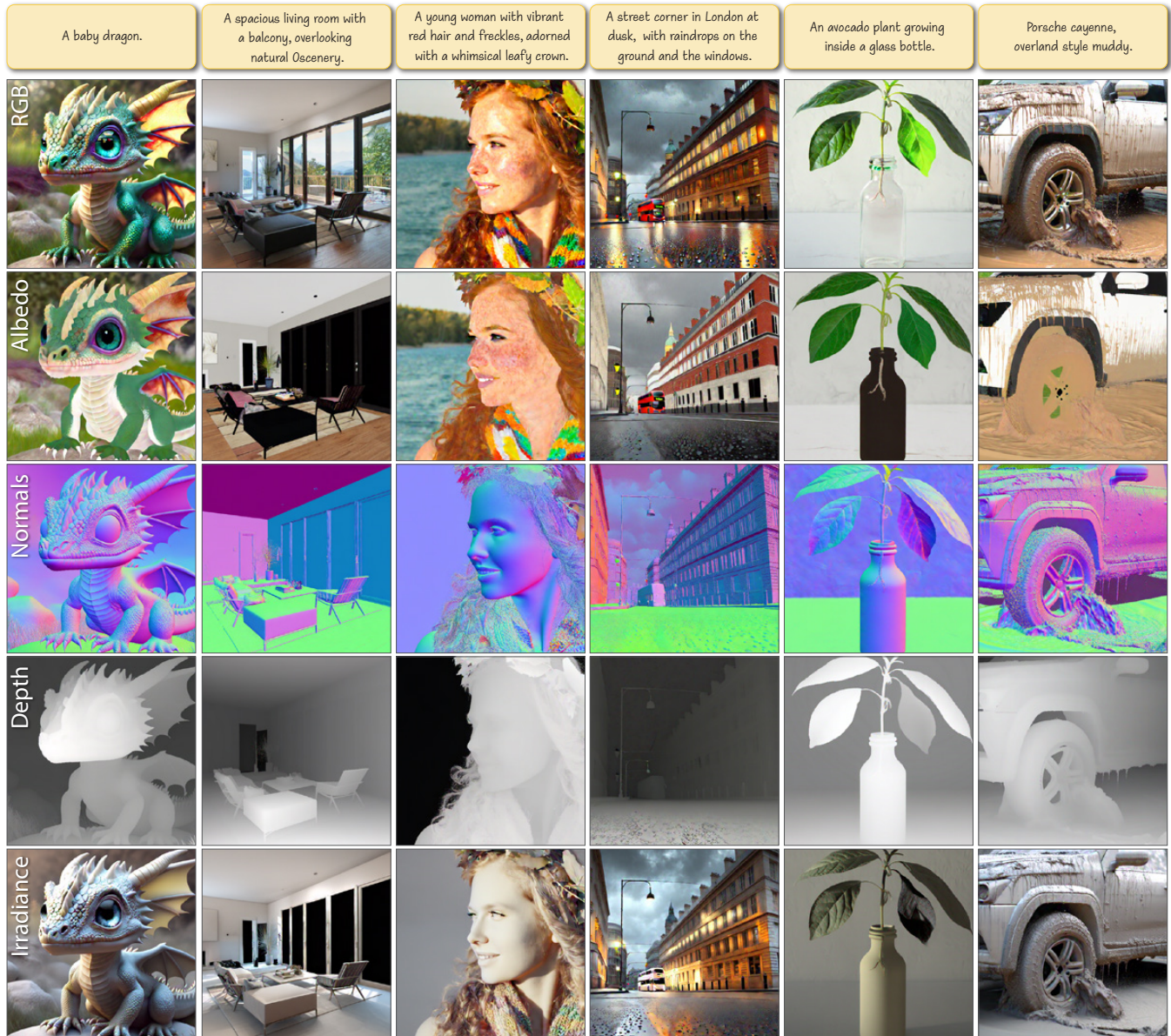


Fig. 11. Text-to-RGB-X samples generated with PRISM. We use MJHQ-30k [Li et al. 2024a] text prompts from various categories to generate diverse samples.

- 10124–10134. <https://api.semanticscholar.org/CorpusID:257427461>
- Tero Karras, Miika Aittala, Samuli Laine, Erik Härkönen, Janne Hellsten, Jaakko Lehtinen, and Timo Aila. 2021. Alias-Free Generative Adversarial Networks. In *Advances in Neural Information Processing Systems (NeurIPS)*.
- Tero Karras, Samuli Laine, and Timo Aila. 2019. A Style-Based Generator Architecture for Generative Adversarial Networks. *Proceedings of the IEEE/CVF Conference on Computer Vision and Pattern Recognition (CVPR)* (2019), 4396–4405. <https://api.semanticscholar.org/CorpusID:54482423>
- Tero Karras, Samuli Laine, Miika Aittala, Janne Hellsten, Jaakko Lehtinen, and Timo Aila. 2020. Analyzing and Improving the Image Quality of StyleGAN. In *Proceedings of the IEEE/CVF Conference on Computer Vision and Pattern Recognition (CVPR)*.
- Bingxin Ke, Anton Obukhov, Shengyu Huang, Nando Metzger, Rodrigo Caye Daudt, and Konrad Schindler. 2024. Repurposing Diffusion-Based Image Generators for

- Monocular Depth Estimation. In *Proceedings of the IEEE/CVF Conference on Computer Vision and Pattern Recognition (CVPR)*.
- Seungryong Kim, Kihong Park, Kwanghoon Sohn, and Stephen Lin. 2016. Unified depth prediction and intrinsic image decomposition from a single image via joint convolutional neural fields. In *Proceedings of the European Conference on Computer Vision (ECCV)*, 143–159.
- Peter Kocsis, Vincent Sitzmann, and Matthias Nießner. 2024. Intrinsic Image Diffusion for Indoor Single-view Material Estimation. *Proceedings of the IEEE/CVF Conference on Computer Vision and Pattern Recognition (CVPR)* (2024), 5198–5208.
- Edwin Herbert Land and John J. McCann. 1971. Lightness and retinex theory. *Journal of the Optical Society of America* 61 1 (1971), 1–11. <https://api.semanticscholar.org/CorpusID:14430259>

- Louis Lettry, Kenneth Vanhoey, and Luc Van Gool. 2018. DARN: a deep adversarial residual network for intrinsic image decomposition. In *IEEE/CVF Winter Conference on Applications of Computer Vision (WACV)*. 1359–1367.
- Daiqing Li, Aleks Kamko, Ehsan Akhgari, Ali Sabet, Linniao Xu, and Suhail Doshi. 2024a. Playground v2.5: Three Insights towards Enhancing Aesthetic Quality in Text-to-Image Generation. *arXiv preprint arXiv:2402.17245* (2024).
- Junnan Li, Dongxu Li, Silvio Savarese, and Steven C. H. Hoi. 2023a. BLIP-2: Bootstrapping Language-Image Pre-training with Frozen Image Encoders and Large Language Models. In *Proceedings of the International Conference on Machine Learning (ICML)*. <https://api.semanticscholar.org/CorpusID:256390509>
- Ming Li, Taojiannan Yang, Huafeng Kuang, Jie Wu, Zhaoning Wang, Xuefeng Xiao, and Chen Chen. 2024c. ControlNet++: Improving Conditional Controls with Efficient Consistency Feedback. In *Proceedings of the European Conference on Computer Vision (ECCV)*. <https://api.semanticscholar.org/CorpusID:269043104>
- Xiang Li, Kai Qiu, Hao Chen, Jason Kuen, Zhe Lin, Rita Singh, and Bhiksha Raj. 2024b. ControlVAR: Exploring Controllable Visual Autoregressive Modeling. *arXiv preprint arXiv:2406.09750* (2024). <https://api.semanticscholar.org/CorpusID:270521423>
- Yuheng Li, Haotian Liu, Qingyang Wu, Fangzhou Mu, Jianwei Yang, Jianfeng Gao, Chunyuan Li, and Yong Jae Lee. 2023b. GLIGEN: Open-Set Grounded Text-to-Image Generation. *Proceedings of the IEEE/CVF Conference on Computer Vision and Pattern Recognition (CVPR)* (2023), 22511–22521. <https://api.semanticscholar.org/CorpusID:255942528>
- Zhengqi Li and Noah Snavely. 2018a. CGIntrinsics: Better Intrinsic Image Decomposition Through Physically-Based Rendering. In *Proceedings of the European Conference on Computer Vision (ECCV)*.
- Zhengqi Li and Noah Snavely. 2018b. Learning intrinsic image decomposition from watching the world. In *Proceedings of the IEEE/CVF Conference on Computer Vision and Pattern Recognition (CVPR)*. 9039–9048.
- Zhengqin Li, Ting-Wei Yu, Shen Sang, Sarah Wang, Meng Song, Yuhua Liu, Yu-Ying Yeh, Rui Zhu, Nitesh Gundavarapu, Jia Shi, Sai Bi, Hong-Xing Yu, Zexiang Xu, Kalyan Sunkavalli, Miloš Hasan, Ravi Ramamoorthi, and Manmohan Chandraker. 2021. OpenRooms: An Open Framework for Photorealistic Indoor Scene Datasets. In *Proceedings of the IEEE/CVF Conference on Computer Vision and Pattern Recognition (CVPR)*.
- Zicheng Liao, Jason Rock, Yang Wang, and David Alexander Forsyth. 2013. Non-parametric Filtering for Geometric Detail Extraction and Material Representation. *Proceedings of the IEEE/CVF Conference on Computer Vision and Pattern Recognition (CVPR)* (2013), 963–970. <https://api.semanticscholar.org/CorpusID:2649952>
- Xiaopei Liu, Lei Jiang, T. Wong, and Chi-Wing Fu. 2012. Statistical Invariance for Texture Synthesis. *IEEE Transactions on Visualization and Computer Graphics (TVCG)* 18 (2012), 1836–1848. <https://api.semanticscholar.org/CorpusID:3165656>
- Yunfei Liu, Yu Li, Shaodi You, and Feng Lu. 2020. Unsupervised learning for intrinsic image decomposition from a single image. In *Proceedings of the IEEE/CVF Conference on Computer Vision and Pattern Recognition (CVPR)*.
- Ilya Loshchilov and Frank Hutter. 2017. Decoupled Weight Decay Regularization. In *International Conference on Learning Representations*. <https://api.semanticscholar.org/CorpusID:53592270>
- Cheng Lu, Yuhao Zhou, Fan Bao, Jianfei Chen, Chongxuan Li, and Jun Zhu. 2022a. DPM-Solver: A Fast ODE Solver for Diffusion Probabilistic Model Sampling in Around 10 Steps. *arXiv preprint arXiv:2206.00927* (2022).
- Cheng Lu, Yuhao Zhou, Fan Bao, Jianfei Chen, Chongxuan Li, and Jun Zhu. 2022b. DPM-Solver++: Fast Solver for Guided Sampling of Diffusion Probabilistic Models. *arXiv preprint arXiv:2211.01095* (2022).
- Jundan Luo, Duygu Ceylan, Jae Shin Yoon, Nanxuan Zhao, Julien Philip, Anna Frühstück, Wenbin Li, Christian Richardt, and Tuanfeng Wang. 2024a. IntrinsicDiffusion: Joint Intrinsic Layers from Latent Diffusion Models. In *ACM SIGGRAPH Conference Proceedings*. Article 74, 11 pages.
- Jundan Luo, Duygu Ceylan, Jae Shin Yoon, Nanxuan Zhao, Julien Philip, Anna Frühstück, Wenbin Li, Christian Richardt, and Tuanfeng Wang. 2024b. IntrinsicDiffusion: Joint Intrinsic Layers from Latent Diffusion Models. In *International Conference on Computer Graphics and Interactive Techniques*. <https://api.semanticscholar.org/CorpusID:271197435>
- Jundan Luo, Zhaoyang Huang, Yijin Li, Xiaowei Zhou, Guofeng Zhang, and Hujun Bao. 2020. NIID-Net: Adapting Surface Normal Knowledge for Intrinsic Image Decomposition in Indoor Scenes. *IEEE Transactions on Visualization and Computer Graphics (TVCG)* 26, 12 (2020), 3434–3445.
- Jundan Luo, Nanxuan Zhao, Wenbin Li, and Christian Richardt. 2023. CRefNet: Learning Consistent Reflectance Estimation With a Decoder-Sharing Transformer. *IEEE Transactions on Visualization and Computer Graphics* (2023).
- Mehdi Mirza and Simon Osindero. 2014. Conditional Generative Adversarial Nets. *arXiv preprint arXiv:1411.1784* (2014). <https://api.semanticscholar.org/CorpusID:12803511>
- Chong Mou, Xintao Wang, Jie Song, Ying Shan, and Jian Zhang. 2023a. DragonDiffusion: Enabling Drag-style Manipulation on Diffusion Models. *arXiv preprint arXiv:2307.02421* (2023). <https://api.semanticscholar.org/CorpusID:259342813>
- Chong Mou, Xintao Wang, Liangbin Xie, Jing Zhang, Zhongang Qi, Ying Shan, and Xiaohu Qie. 2023b. T2I-Adapter: Learning Adapters to Dig out More Controllable Ability for Text-to-Image Diffusion Models. *arXiv preprint arXiv:2302.08453* (2023). <https://api.semanticscholar.org/CorpusID:256900833>
- Takuya Narihira, Michael Maire, and Stella X Yu. 2015. Learning lightness from human judgement on relative reflectance. In *Proceedings of the IEEE/CVF Conference on Computer Vision and Pattern Recognition (CVPR)*. 2965–2973.
- Alex Nichol, Pratul Dharwal, Aditya Ramesh, Pranav Shyam, Pamela Mishkin, Bob McGrew, Ilya Sutskever, and Mark Chen. 2021. GLIDE: Towards Photorealistic Image Generation and Editing with Text-Guided Diffusion Models. In *Proceedings of the International Conference on Machine Learning (ICML)*.
- Xichen Pan, Li Dong, Shaohan Huang, Zhiliang Peng, Wenhui Chen, and Furu Wei. 2023. Kosmos-G: Generating Images in Context with Multimodal Large Language Models. *arXiv preprint arXiv:2310.02992* (2023). <https://api.semanticscholar.org/CorpusID:263620748>
- Foivos Paraperas Papantoniou, Alexandros Lattas, Stylianos Moschoglou, Jiankang Deng, Bernhard Kainz, and Stefanos Zafeiriou. 2024. Arc2Face: A Foundation Model for ID-Consistent Human Faces. *Proceedings of the European Conference on Computer Vision (ECCV)* (2024).
- William S. Peebles and Saining Xie. 2022. Scalable Diffusion Models with Transformers. *Proceedings of the IEEE/CVF International Conference on Computer Vision (ICCV)* (2022), 4172–4182. <https://api.semanticscholar.org/CorpusID:254854389>
- Zhiliang Peng, Wenhui Wang, Li Dong, Yaru Hao, Shaohan Huang, Shuming Ma, and Furu Wei. 2023. Kosmos-2: Grounding Multimodal Large Language Models to the World. *arXiv preprint arXiv:2306.14824* (2023). <https://api.semanticscholar.org/CorpusID:259262263>
- Alec Radford, Jong Wook Kim, Chris Hallacy, Aditya Ramesh, Gabriel Goh, Sandhini Agarwal, Girish Sastry, Amanda Askell, Pamela Mishkin, Jack Clark, Gretchen Krueger, and Ilya Sutskever. 2021. Learning Transferable Visual Models From Natural Language Supervision. In *Proceedings of the International Conference on Machine Learning (ICML)*. <https://api.semanticscholar.org/CorpusID:231591445>
- Colin Raffel, Noam M. Shazeer, Adam Roberts, Katherine Lee, Sharan Narang, Michael Matena, Yanqi Zhou, Wei Li, and Peter J. Liu. 2019. Exploring the Limits of Transfer Learning with a Unified Text-to-Text Transformer. *Journal of Machine Learning Research (JMLR)* 21 (2019), 140:1–140:67. <https://api.semanticscholar.org/CorpusID:204838007>
- Aditya Ramesh, Pratul Dharwal, Alex Nichol, Casey Chu, and Mark Chen. 2022. Hierarchical Text-Conditional Image Generation with CLIP Latents. *arXiv preprint arXiv:2204.06125* (2022).
- Aditya Ramesh, Mikhail Pavlov, Gabriel Goh, Scott Gray, Chelsea Voss, Alec Radford, Mark Chen, and Ilya Sutskever. 2021. Zero-shot text-to-image generation. In *Proceedings of the International Conference on Machine Learning (ICML)*.
- René Ranftl, Alexey Bochkovskiy, and Vladlen Koltun. 2021. Vision Transformers for Dense Prediction. *ArXiv preprint* (2021).
- René Ranftl, Katrin Lasinger, David Hafner, Konrad Schindler, and Vladlen Koltun. 2019. Towards Robust Monocular Depth Estimation: Mixing Datasets for Zero-Shot Cross-Dataset Transfer. *IEEE Transactions on Pattern Analysis and Machine Intelligence* 44 (2019), 1623–1637. <https://api.semanticscholar.org/CorpusID:195776274>
- René Ranftl, Katrin Lasinger, David Hafner, Konrad Schindler, and Vladlen Koltun. 2022. Towards Robust Monocular Depth Estimation: Mixing Datasets for Zero-Shot Cross-Dataset Transfer. *IEEE Transactions on Pattern Analysis and Machine Intelligence* 44, 3 (2022).
- Scott E. Reed, Zeynep Akata, Xichen Yan, Lajanugen Logeswaran, Bernt Schiele, and Honglak Lee. 2016. Generative Adversarial Text to Image Synthesis. In *Proceedings of the International Conference on Machine Learning (ICML)*. <https://api.semanticscholar.org/CorpusID:1563370>
- Mike Roberts, Jason Ramapuram, Anurag Ranjan, Atulit Kumar, Miguel Angel Bautista, Nathan Paczan, Russ Webb, and Joshua M Susskind. 2021a. Hypersim: A photorealistic synthetic dataset for holistic indoor scene understanding. In *Proceedings of the IEEE/CVF International Conference on Computer Vision (ICCV)*. 10912–10922.
- Mike Roberts, Jason Ramapuram, Anurag Ranjan, Atulit Kumar, Miguel Angel Bautista, Nathan Paczan, Russ Webb, and Joshua M. Susskind. 2021b. Hypersim: A Photorealistic Synthetic Dataset for Holistic Indoor Scene Understanding. In *Proceedings of the IEEE/CVF International Conference on Computer Vision (ICCV)*.
- Robin Rombach, A. Blattmann, Dominik Lorenz, Patrick Esser, and Björn Ommer. 2021. High-Resolution Image Synthesis with Latent Diffusion Models. *Proceedings of the IEEE/CVF Conference on Computer Vision and Pattern Recognition (CVPR)* (2021), 10674–10685.
- Nataniel Ruiz, Yuanzhen Li, Varun Jampani, Yael Pritch, Michael Rubinstein, and Kfir Aberman. 2022. DreamBooth: Fine Tuning Text-to-Image Diffusion Models for Subject-Driven Generation. *Proceedings of the IEEE/CVF Conference on Computer Vision and Pattern Recognition (CVPR)* (2022), 22500–22510. <https://api.semanticscholar.org/CorpusID:251800180>
- Chitwan Saharia, William Chan, Saurabh Saxena, Lala Li, Jay Whang, Emily L. Denton, Seyed Kamyar Seyed Ghasemipour, Burcu Karagol Ayan, Seyedeh Sara Mahdavi, Raphael Gontijo Lopes, Tim Salimans, Jonathan Ho, David J. Fleet, and Mohammad Norouzi. 2022. Photorealistic Text-to-Image Diffusion Models with Deep Language Understanding. *arXiv preprint arXiv:2205.11487* (2022).

- Tim Salimans, Ian J. Goodfellow, Wojciech Zaremba, Vicki Cheung, Alec Radford, and Xi Chen. 2016. Improved Techniques for Training GANs. *arXiv preprint arXiv:1606.03498* (2016). <https://api.semanticscholar.org/CorpusID:1687220>
- Thomas Schöps, Johannes L. Schönberger, Silvano Galliani, Torsten Sattler, Konrad Schindler, Marc Pollefeys, and Andreas Geiger. 2017. A Multi-view Stereo Benchmark with High-Resolution Images and Multi-camera Videos. *2017 IEEE Conference on Computer Vision and Pattern Recognition (CVPR)* (2017), 2538–2547. <https://api.semanticscholar.org/CorpusID:20603040>
- Nathan Silberman, Derek Hoiem, Pushmeet Kohli, and Rob Fergus. 2012. Indoor Segmentation and Support Inference from RGBD Images. In *European Conference on Computer Vision*. <https://api.semanticscholar.org/CorpusID:545361>
- Jiaming Song, Chenlin Meng, and Stefano Ermon. 2020. Denoising Diffusion Implicit Models. *arXiv preprint arXiv:2010.02502* (2020).
- Roman Suvorov, Elizaveta Logacheva, Anton Mashikhin, Anastasia Remizova, Arsenii Ashukha, Aleksei Silvestrov, Naejin Kong, Harshith Goka, Kiwoong Park, and Victor S. Lempitsky. 2021. Resolution-robust Large Mask Inpainting with Fourier Convolutions. *IEEE/CVF Winter Conference on Applications of Computer Vision (WACV)* (2021), 3172–3182.
- Ming Tao, Hao Tang, Fei Wu, Xiao-Yuan Jing, Bing-Kun Bao, and Changsheng Xu. 2022. DF-GAN: A Simple and Effective Baseline for Text-to-Image Synthesis. In *Proceedings of the IEEE/CVF Conference on Computer Vision and Pattern Recognition (CVPR)*.
- Marshall F. Tappen, Edward H. Adelson, and William T. Freeman. 2006. Estimating Intrinsic Component Images using Non-Linear Regression. *Proceedings of the IEEE/CVF Conference on Computer Vision and Pattern Recognition (CVPR)* 2 (2006), 1992–1999. <https://api.semanticscholar.org/CorpusID:12373622>
- Marshall F. Tappen, William T. Freeman, and Edward H. Adelson. 2005. Recovering intrinsic images from a single image. *IEEE Transactions on Pattern Analysis and Machine Intelligence (TPAMI)* 27 (2005), 1459–1472. <https://api.semanticscholar.org/CorpusID:801056>
- Wenhai Wang, Enze Xie, Xiang Li, Deng-Ping Fan, Kaitao Song, Ding Liang, Tong Lu, Ping Luo, and Ling Shao. 2022. Pvt v2: Improved baselines with pyramid vision transformer. *Computational Visual Media* 8, 3 (2022), 415–424.
- Jiaye Wu, Sanjoy Chowdhury, Hariharmano Shanmugaraja, David Jacobs, and Soumyadip Sengupta. 2023. Measured Albedo in the Wild: Filling the Gap in Intrinsic Evaluation. *2023 IEEE International Conference on Computational Photography (ICCP)* (2023), 1–12. <https://api.semanticscholar.org/CorpusID:259262357>
- Weihao Xia, Yujia Yang, Jing Xue, and Baoyuan Wu. 2021. TediGAN: Text-Guided Diverse Face Image Generation and Manipulation. *Proceedings of the IEEE/CVF Conference on Computer Vision and Pattern Recognition (CVPR)* (2021), 2256–2265. <https://api.semanticscholar.org/CorpusID:235702618>
- Shitao Xiao, Yueze Wang, Junjie Zhou, Huaying Yuan, Xingrun Xing, Ruiran Yan, Shutong Wang, Tiejun Huang, and Zheng Liu. 2024. OmniGen: Unified Image Generation. *arXiv preprint arXiv:2409.11340* (2024). <https://api.semanticscholar.org/CorpusID:272694523>
- Tao Xu, Pengchuan Zhang, Qiuyuan Huang, Han Zhang, Zhe Gan, Xiaolei Huang, and Xiaodong He. 2018. AttnGAN: Fine-grained text to image generation with attentional generative adversarial networks. In *Proceedings of the IEEE/CVF Conference on Computer Vision and Pattern Recognition (CVPR)*.
- Lihe Yang, Bingyi Kang, Zilong Huang, Xiaogang Xu, Jiashi Feng, and Hengshuang Zhao. 2024a. Depth Anything: Unleashing the Power of Large-Scale Unlabeled Data. In *CVPR*.
- Lihe Yang, Bingyi Kang, Zilong Huang, Zhen Zhao, Xiaogang Xu, Jiashi Feng, and Hengshuang Zhao. 2024b. Depth Anything V2. *arXiv:2406.09414* (2024).
- Ziyu Yao, Jialin Li, Yifeng Zhou, Yong Liu, Xi Jiang, Chengjie Wang, Feng Zheng, Yuxian Zou, and Lei Li. 2024. CAR: Controllable Autoregressive Modeling for Visual Generation. *arXiv preprint arXiv:2410.04671* (2024). <https://api.semanticscholar.org/CorpusID:273186014>
- Chongjie Ye, Lingteng Qiu, Xiaodong Gu, Qi Zuo, Yushuang Wu, Zilong Dong, Liefeng Bo, Yuliang Xiu, and Xiaoguang Han. 2024. StableNormal: Reducing Diffusion Variance for Stable and Sharp Normal. *ACM Transactions on Graphics (ToG)* (2024).
- Hu Ye, Jun Zhang, Siyi Liu, Xiao Han, and Wei Yang. 2023. IP-Adapter: Text Compatible Image Prompt Adapter for Text-to-Image Diffusion Models. *arXiv preprint arXiv:2308.06721* (2023). <https://api.semanticscholar.org/CorpusID:260886966>
- Wei Yin, Yifan Liu, and Chunhua Shen. 2021. Virtual Normal: Enforcing Geometric Constraints for Accurate and Robust Depth Prediction. *IEEE Transactions on Pattern Analysis and Machine Intelligence (TPAMI)* (2021).
- Wei Yin, Jianming Zhang, Oliver Wang, Simon Niklaus, Long Mai, Simon Chen, and Chunhua Shen. 2020. Learning to Recover 3D Scene Shape from a Single Image. *2021 IEEE/CVF Conference on Computer Vision and Pattern Recognition (CVPR)* (2020), 204–213. <https://api.semanticscholar.org/CorpusID:229298063>
- Jiahui Yu, Yuanzhong Xu, Jing Yu Koh, Thang Luong, Gunjan Baid, Zirui Wang, Vijay Vasudevan, Alexander Ku, Yinfei Yang, Burcu Karagol Ayan, et al. 2022. Scaling autoregressive models for content-rich text-to-image generation. *arXiv preprint arXiv:2206.10789* (2022).
- Zheng Zeng, Valentin Deschaintre, Iliyan Georgiev, Yannick Hold-Geoffroy, Yiwei Hu, Fujun Luan, Ling-Qi Yan, and Miloš Hašan. 2024. RGB \leftrightarrow X: Image decomposition and synthesis using material- and lighting-aware diffusion models. In *ACM SIGGRAPH Conference Proceedings*. Article 75, 11 pages.
- Chi Zhang, Wei Yin, Zhibin Wang, Gang Yu, Bin Fu, and Chunhua Shen. 2022. Hierarchical Normalization for Robust Monocular Depth Estimation. *NeurIPS* (2022).
- Han Zhang, Tao Xu, Hongsheng Li, Shaoting Zhang, Xiaogang Wang, Xiaolei Huang, and Dimitris N Metaxas. 2017. StackGAN: Text to photo-realistic image synthesis with stacked generative adversarial networks. In *Proceedings of the IEEE/CVF International Conference on Computer Vision (ICCV)*.
- Lymin Zhang, Anyi Rao, and Maneesh Agrawala. 2023. Adding Conditional Control to Text-to-Image Diffusion Models. *Proceedings of the IEEE/CVF International Conference on Computer Vision (ICCV)* (2023), 3813–3824. <https://api.semanticscholar.org/CorpusID:256827727>
- Richard Zhang, Phillip Isola, Alexei A. Efros, Eli Shechtman, and Oliver Wang. 2018b. The Unreasonable Effectiveness of Deep Features as a Perceptual Metric. *Proceedings of the IEEE/CVF Conference on Computer Vision and Pattern Recognition (CVPR)* (2018), 586–595. <https://api.semanticscholar.org/CorpusID:4766599>
- Zhicheng Zhang, Guangzhe Dai, Xiaokun Liang, Shaode Yu, Leida Li, and Yaoqin Xie. 2018a. Can signal-to-noise ratio perform as a baseline indicator for medical image quality assessment. *IEEE Access* 6 (2018), 11534–11543.
- Canyu Zhao, Mingyu Liu, Huanyi Zheng, Muzhi Zhu, Zhiyue Zhao, Hao Chen, Tong He, and Chunhua Shen. 2025. DICEPTION: A Generalist Diffusion Model for Visual Perceptual Tasks. *ArXiv abs/2502.17157* (2025). <https://api.semanticscholar.org/CorpusID:276575582>
- Qi Zhao, Ping Tan, Qiang Dai, Li Shen, Enhua Wu, and Stephen Lin. 2012. A Closed-Form Solution to Retinex with Nonlocal Texture Constraints. *IEEE Transactions on Pattern Analysis and Machine Intelligence (TPAMI)* 34 (2012), 1437–1444. <https://api.semanticscholar.org/CorpusID:2277868>
- Shihao Zhao, Dongdong Chen, Yen-Chun Chen, Jianmin Bao, Shaozhe Hao, Lu Yuan, and Kwan-Yee K. Wong. 2023. Uni-ControlNet: All-in-One Control to Text-to-Image Diffusion Models. *arXiv preprint arXiv:2305.16322* (2023). <https://api.semanticscholar.org/CorpusID:258888112>
- Hao Zhou, Xiang Yu, and David W Jacobs. 2019. GLoSH: Global-Local Spherical Harmonics for Intrinsic Image Decomposition. In *Proceedings of the IEEE/CVF International Conference on Computer Vision (ICCV)*. 7820–7829.
- Tinghui Zhou, Philipp Krähenbühl, and Alexei A Efros. 2015. Learning data-driven reflectance priors for intrinsic image decomposition. In *Proceedings of the IEEE/CVF International Conference on Computer Vision (ICCV)*. 3469–3477.
- Jingsen Zhu, Fujun Luan, Yuchi Huo, Zihao Lin, Zhihua Zhong, Dianbing Xi, Rui Wang, Hujun Bao, Jiaxiang Zheng, and Rui Tang. 2022. Learning-Based Inverse Rendering of Complex Indoor Scenes with Differentiable Monte Carlo Raytracing. In *ACM SIGGRAPH Asia Conference Proceedings*. ACM, Article 6, 8 pages. <https://doi.org/10.1145/3550469.3555407>
- Minfeng Zhu, Pingbo Pan, Wei Chen, and Yi Yang. 2019. Dm-GAN: Dynamic memory generative adversarial networks for text-to-image synthesis. In *Proceedings of the IEEE/CVF Conference on Computer Vision and Pattern Recognition (CVPR)*.
- Daniel Zoran, Phillip Isola, Dilip Krishnan, and William T Freeman. 2015. Learning ordinal relationships for mid-level vision. In *Proceedings of the IEEE/CVF International Conference on Computer Vision (ICCV)*.